Subpicosecond luminescence rise time in magnesium codoped GAGG:Ce scintillator

G. Tamulaitis [a],*, A. Vaitkevičius [a], S. Nargelas [a], R. Augulis [b], V. Gulbinas [b], P. Bohacek [c], M. Nikl [c], A. Borisevich [d], A. Fedorov [d], M. Korjik [d], E. Auffray [e]

[a] Institute of Applied Research and Semiconductor Physics Department, Vilnius University, Saulėtekio al. 3, LT-10257, Vilnius, Lithuania
[b] Center for Physical Sciences and Technology, Saulėtekio al. 3, LT-10257, Vilnius, Lithuania
[c] Institute of Physics CAS, Cukrovarnicka 10, Prague, Czech Republic
[d] Research Institute for Nuclear Problems, Bobruiskaya str. 11, Minsk, Belarus
[e] CERN, Geneva, Switzerland

A B S T R A C T

The influence of co-doping of $Gd_3Al_2GA_3O_{12}$:Ce (GAGG:Ce) scintillator with magnesium on the rise time of luminescence response was studied in two GAGG:Ce crystals grown in nominally identical conditions except of Mg co-doping in one of them. Time-resolved photoluminescence spectroscopy and free carrier absorption techniques were exploited. It is evidenced that the Mg co-doping decreases the rise time down to sub-picosecond domain. Meanwhile, the light yield decreases by ∼20%. Thus, the feasibility of exploitation of the fast rise edge in luminescence response for ultrafast timing in scintillation detectors is demonstrated. The role of Mg impurities in facilitating the excitation transfer to radiative recombination centers is discussed.

1. Introduction

The improvement of time resolution down to ∼10 ps is currently one of the hottest topics in the development of radiation detectors based on scintillation crystals [1]. The fast detector response is necessary to prevent the pile-up effect in high-luminosity high-energy physics experiments [2] as well as to enable the decrease of the dose injected to a patient in medical imaging, in particular, in time-of-flight positron emission tomography (TOF-PET) [3] and positron annihilation lifetime spectroscopy (PALS) [4]. Recent advances in photodetectors, especially in silicon multipliers (SiPMs) [5] resulted in a substantial shift of the frontiers in the development of fast photon counting devices towards the 10 ps target. Thus, the response time of bulk scintillation crystals currently becomes the bottleneck in the time resolution of the radiation detectors based on the scintillators. The currently fastest scintillation detectors are based on BaF_2, $LaBr_3$:Ce, $CeBr_3$, Pr-doped oxides [6], Ca-codoped LSO:Ce [7] and LYSO:Ce [8], and also trivalent-ion doped PWO [9]. To study the capability of scintillators to serve in fast radiation detectors, not only the emission decay time but also the rise time of their luminescence response is being currently reinvestigated. It is demonstrated that the scintillation rise time in many LSO-type scintillators is 70 ps, while LSO:Ce co-doped with Ca is expected to

exhibit the rise time of 20 ps [10]. A sub-picosecond photoluminescence (PL) rise time is revealed in conventional PWO II scintillation crystals, while the PL response to short-pulse excitation takes a few nanoseconds in a solely Ce-doped gadolinium aluminum gallium garnet ($Gd_3Al_2Ga_3O_{12}$:Ce, GAGG:Ce) [11].

Due to a high light yield of up to 50000 ph/MeV, a short luminescence decay time (< 100 ns) [12], and good matching of the emission band with the sensitivity spectrum of conventional SiPMs, GAGG:Ce is a promising scintillation material for certain particle physics experiments and might compete with Ce-doped LYSO and LSO crystals in TOF-PETs. Therefore, the luminescence rise time of this scintillator is of special importance. On the other hand, co-doping of GAGG:Ce by Mg results in a significant improvement of timing characteristics [13] and especially of the coincidence time resolution down to 233 ps due to faster rise and decay times of the scintillation response [14] and paves an efficient way for reaching a better time resolution in detectors based on this material. Moreover, the capability of reaching the time resolution below 50 ps, was demonstrated in GAGG:Ce,Mg thin crystals at the excitation with a high energy charged pion beam [15]. Meanwhile, the origin of the luminescence rise time shortening in Mg-codoped GAGG:Ce is still not unambiguously understood. A lack of information on scintillation kinetics in a

---

picosecond domain is one of the key problems. Better understanding of the mechanism of the scintillation build-up acceleration in magnesium codoped garnet crystal might be useful for the future improvement of the technology for growing mixed garnet scintillation crystals.

The study of the details of the luminescence kinetics in a ps-sub-ps domain is hardly feasible by using X-ray or particle beam sources and conventional coincidence technique. To investigate the excitation transfer in this time domain, we used excitation by femtosecond UV laser pulses. The luminescence response to the excitation by 80-fs-long pulses was studied using streak camera. To compare the PL response kinetics with the time evolution of the density of nonequilibrium carriers, free carrier absorption (FCA) has been also investigated in these two samples by using pump and probe configuration ensuring sub-picosecond time resolution.

2. Experimental

The samples under study were grown at the Institute of Physics, Czech Academy of Sciences, by the Czochralski method from iridium crucibles. Both samples were intentionally grown in nominally identical conditions except that the sample GAGG:Ce was doped only by 0.5 at% of cerium, while the sample GAGG:Ce, Mg was additionally co-doped with magnesium by adding 0.1 at.% of Mg into the melt. The samples were cut from single crystal boules in a shape of a block with dimensions of $3 \times 3 \times 5$ mm^3 and polished. The light yield of the samples was measured by using a photomultiplier tube (PMT) with bialkali photocathode and 1×1 inch CsI(Tl) reference crystal and found to be 35,000 ph/MeV and 27,000 ph/MeV for GAGG:Ce and GAGG:Ce,Mg, respectively.

The time-resolved photoluminescence (TRPL) study has been performed by using a Hamamatsu streak camera. A femtosecond Yb:KGW oscillator (Light Conversion Ltd.) emitting 65 fs pulses at 76 MHz repetition rate was used for excitation. The oscillator emission at 1030 nm was converted to the third 343 nm (3.64 eV) and fourth 254 nm (4.9 eV) harmonics by a harmonics generator (HIRO, Light Conversion Ltd.). The time resolution in these experiments was determined by the instrumental response function of the streak camera. In synchroscan operation mode, the best time resolution was limited by the instrumental response function with full width at half maximum (FWHM) of 3.38 ps.

The decay of nonequilibrium carriers was also investigated by studying free carrier absorption (FCA). Pump and probe configuration was used in these experiments. The free carriers were generated by 200-fs-long pump pulses with photon energy of 4.9 eV (254 nm). The fourth harmonic of the Yb:KGW laser radiation was generated for the pump from a fraction of the fundamental harmonic using β-barium borate crystals. The optical absorption of the samples was probed in the infrared region. The probe pulses were generated in a parametric generator at fixed wavelengths in the range from 1040 to 1712 nm (1.2 eV–0.73 eV). The variable delay of the probe beam enabled time-resolved measurements of free carrier absorption. The differential absorption (DA), i.e., the difference in the optical absorption observed with and without the pump was measured as a function of the delay between the pump and probe pulses. The DA in infrared region is caused predominantly by the free carrier absorption. Thus, the absolute value of DA is proportional to free carrier density.

All the measurements were performed at room temperature.

3. Results and discussion

The absorbance spectra of the samples GAGG:Ce and GAGG:Ce,Mg in the spectral range under study are presented in Fig. 1. They are dominated by the absorption bands due to optical transitions in Ce^{3+} ions: 4f-5d^1 at 2.79 eV and 4f-5d^2 at 3.64 eV. Co-doping by Mg results in unstructured enhancement of the absorption in the high-energy part of the spectrum. The absorption in this spectral region might be attributed to the broad band due to the charge transfer transition of Ce^{4+} stabilized by aliovalent doping of divalent magnesium [15,16], though the close
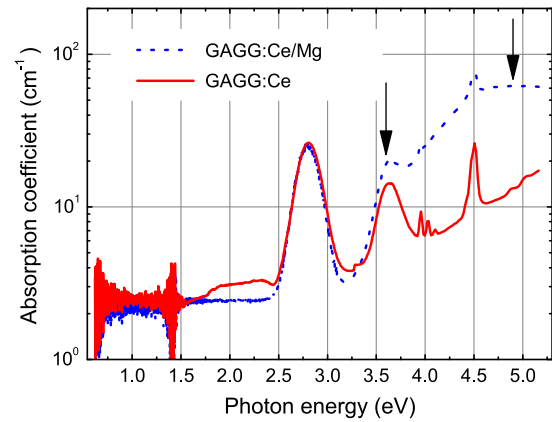

Fig. 1. (Color online) Room temperature absorption spectra of samples GAGG:Ce (red solid line) and GAGG:Ce.Mg (blue dotted line).

values of the absorption coefficients in the band due to 4f-5d^1 transition in both samples shows that only a small part of Ce^{3+} is converted into Ce^{4+} state in the co-doped crystal. The sharp lines around 4 eV and 4.5 eV are due to the electronic transitions from ^{8}S ground state to higher ^{6}P and ^{6}I 4f states in Gd^{3+} ions. The co-doping does not affect the positions of the absorption bands caused by cerium, thus, the crystal field in the vicinity of Ce^{3+} ions is not affected by the introduction of magnesium. In addition, a wide absorption band in the range from 1.8 eV to 2.5 eV is strongly suppressed by the Mg codoping. The broad absorption band was observed in garnet type crystals at low doping level [17] and most probably is caused by structural imperfection of the host matrix.

The activator luminescence spectra of both samples under study are identical within the limits of experimental error and are described elsewhere [11–13]. The spectrum has the shape of two strongly overlapping broad bands caused by transitions from 5d^1 excited state to ^{2}F$_{5/2}$ and ^{2}F$_{7/2}$ ground state doublet of Ce^{3+} ion [12]. The excitation at 254 nm produces also a weak and narrow Gd^{3+} emission band with the peak position at 318 nm and the intensity of two orders of magnitude weaker than that of activator luminescence. The similarity of the activator spectra in GAGG:Ce without and with codoping evidences negligible influence of Mg co-doping on the emission mechanism. Therefore, the influence of the Mg co-doping on the dynamics of nonequilibrium charge carriers and, consequently, on the emission kinetics might be expected via the impact on the transport of the nonequilibrium carriers to radiative recombination centers, i.e., Ce^{3+} ions.

The luminescence kinetics was studied by using time-resolved photoluminescence spectroscopy. To selectively excite predominantly Ce^{3+} and Gd^{3+} ions, two photon energies were selected for the photoluminescence excitation. They are indicated by arrows in Fig. 1. The photons of the third harmonic at 3.6 eV (343 nm) excite Ce^{3+} ion into the second Stark component of 5d excited energy level. The photon energy of the fourth harmonic at 4.9 eV (254 nm) corresponds to the energy of ^{8}S→^{6}D$_{7/2,9/2}$ transitions in Gd^{3+} ions and to the long wavelength wing of the absorption band due to optical transition to the third Stark component of 4f^{0}5d^1 Ce^{3+} electronic configuration overlapping with a broad band, which is probably caused by charge transfer absorption of Ce^{4+} in the crystal co-doped with magnesium. It is worth noting that the second Stark component of 5d level of Ce^{3+} in GAGG host is situated already in its conduction band [18–20], which enables electron escape from this level to the host conduction band and activates trapping–retrapping processes giving rise to a delayed radiative recombination at Ce^{3+} ions.

The initial part of the photoluminescence response to the same short pulse excitation (65 fs) is presented in Fig. 2 for both samples under study. The instrumental response functions are also presented in the
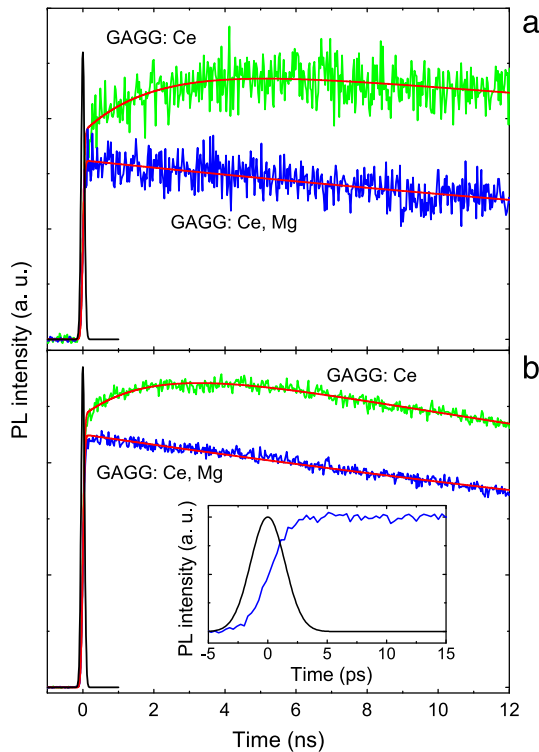
Fig. 2. (Color online) The initial part of photoluminescence response to a short excitation pulse 254 nm (a) and 343 nm (b) of GAGG:Ce and GAGG:Ce,Mg (indicated). Instrumental response function is also presented (black). Inset shows the rising part of the luminescence response in GAGG:Ce,Mg.
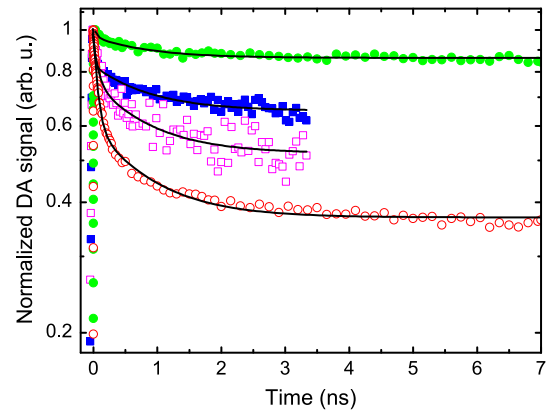

Fig. 3. (Color online) Kinetics of normalized differential absorption for pumping at 4.9 eV in GAGG:Ce (filled circles) and GAGG:Ce,Mg (open circles) and at 5.8 eV in GAGG:Ce (filled squares) and GAGG:Ce,Mg (open squares). All the transients were probed at 1.2 eV. The lines present bi-exponential fits of experimental kinetics.

figure. The deconvolution of the instrumental response function and the luminescence response in the kinetics of GAGG:Ce luminescence after excitation at 3.64 eV (343 nm) shows that the response has two rise components. The first component is faster than the instrumental response function, while the second component has the time constant of 2 ns. The luminescence decays with the time constant of 47 ns (see Fig. 2(a)). The kinetics after 4.9 eV (254 nm) excitation is similar. The presence of the relatively long luminescence rise component seems to be caused by involvement of Gd subsystem: a part of the nonequilibrium electrons are trapped by shallow traps and are captured afterwards by deeper Gd^{3+} levels, which have poor resonance with Ce^{3+} excited state. The rising part of the GAGG:Ce,Mg was irresolvable within the time resolution in our experiment, while the decay was fitted with a single exponential decay with 48.3 ns time constant. In both cases, the experimental data was considered to be a convolution of the photoluminescence response and a Gaussian function with 110 ps FWHM, which closely matches the instrumental response function in our experiments. To resolve the luminescence rise of GAGG:Ce,Mg, the very initial part of the luminescence response was measured (see inset in Fig. 2) with considerably better time resolution ensured by the instrumental response function with FWHM of 3.4 ps. Even at this accuracy, the rising part of the luminescence response could not be quantified, i.e., the rising part of the response is in a sub-picosecond domain. The absence of the slow component in the build-up of photoluminescence response of the Mg-codoped sample is caused by the increased rate of repopulation of Ce^{3+} radiative recombination centers by electrons released from Ce^{3+} 5d level, which is in conduction band. The process might be facilitated by the presence of stable Ce^{4+} centers which effectively attract electrons and enable their immediate nongeminate radiative recombination giving rise to prompt Ce^{3+} luminescence or by introduction of Mg-based defect states in the band gap attracting electrons from shallow traps and supplying them to the radiative Ce^{3+} centers via Gd^{3+} subsystem.

To get a deeper insight into the dynamics of nonequilibrium carriers, the kinetics of differential absorption were studied in GAGG:Ce and GAGG:Ce,Mg for two pump photon energies, 4.9 eV and 5.8 eV (see Fig. 3). The pump photons of 4.9 eV are in resonance with the optical transition to the third excited state of Ce^{3+}, while they are also able to excite the matrix-building Gd^{3+} ions. The pump photon energy of 5.8 eV is still below the band gap of GAGG matrix but is sufficient to excite the electrons from the valence band to the trap states closely below the bottom of the conduction band. The 5.8 eV photons might also excite the activator ion Ce^{3+} to unlocalized states high in the conduction band. The FCA transients in Fig. 3 are presented in a normalized form to better compare their time evolution in the crystals with and without codoping and at different excitation conditions. All the transients have qualitatively the same shape: a short initial decay transforming into a considerably slower decay at longer delays. The decay times of the components are quite similar, but the relative contribution of the components is sensitive to codoping and depends on excitation wavelength. The smallest contribution (and the longest decay time of 268 ps that was determined with a large error due to small weight of this component) is observed in GAGG:Ce excited at 4.9 eV. Mg-codoping results in substantial enhancement of the fast component (68 ps). For excitation at 5.8 eV, the fast component in GAGG:Ce (58 ps) is stronger than that at 4.9 eV, while Mg-codoping increases the contribution of the fast component (79 ps), though not so strong as at 4.9 eV.

In Fig. 4, the PL kinetics (depicted in Fig. 2) are compared with the time evolution of FCA transients at 4.9 eV pump (depicted in Fig. 3) in the same two samples. The FCA curves represent the difference in absorbance of the probe beam (the photon energy of 1.20 eV) with and without the pump beam. The differential absorption in this spectral region is proportional to the density of free carriers. The results presented above are consistent with the assumption that the absorption of nonequilibrium holes is dominating over the absorption of nonequilibrium electrons in FCA of GAGG:Ce [21]. First of all, this assumption is confirmed by the results obtained at 4.9 eV excitation. The pump photons of 4.9 eV might be absorbed by Ce^{3+} to the third excited state as well as by Gd^{3+} ions in the crystal lattice. The second absorption channel should be stronger due to a high density of the matrix-building Gd^{3+} ions. Moreover, the excited states of the radiative Ce^{3+} ions are in the conduction band. Therefore, the population of electrons at excited Ce^{3+}, which determines the luminescence, and their population in conduction band, which is reflected in the FCA signal due to free electrons, should be in equilibrium. Instead, we observe an initial rise in luminescence intensity but a decrease in FCA (see Fig. 4) for approximately 1 ns after short-pulse excitation that is by far longer than the time necessary to establish the equilibrium. Thus, the FCA signal
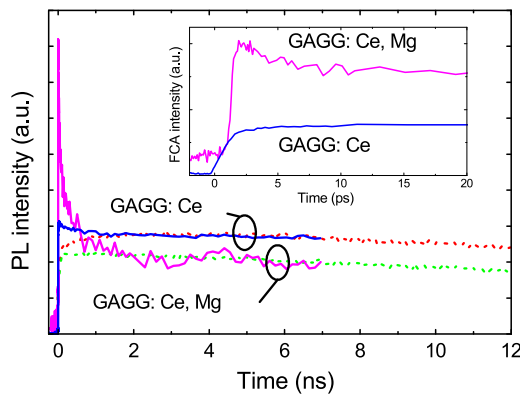
Fig. 4. (Color online) Kinetics of photoluminescence intensity (dotted curves), as in Fig. 2, and free carrier absorption (solid curves), as in Fig. 3, in GAGG:Ce and GAGG:Ce,Mg, as indicated. FCA curves are arbitrary shifted to match the PL curves at the late decay stage. The inset expands the initial part of the free carrier absorption kinetics.

in GAGG:Ce reflects the time evolution of free holes rather than that of free electrons. This conclusion is also supported by the qualitatively different behavior of FCA, which has previously been observed in Ce-doped YAGG, a garnet without gadolinium [21].

The strong enhancement of the fast decay component in FCA by Mg-codoping at predominant excitation of Gd^{3+} shows that the Mg doping introduces nonradiative recombination centers with rather strong coupling of the centers with Gd^{3+}. Thus, the Mg-codoping facilitates the excitation transfer from gadolinium sublattice to the radiative Ce^{3+} centers but simultaneously enhances nonradiative recombination and, consequently, decreases the light yield. The influence of the nonradiative recombination centers introduced by Mg-doping is weaker at 5.8 eV excitation (the fast component in Fig. 3 is less affected by Mg-codoping). It is worth noting that the decrease in the light yield of GAGG:Ce by ∼20%, which we observed in the Mg-codoped sample under study, is still acceptable for many applications of GAGG:Ce,Mg as a fast scintillator.

In nanosecond domain, the decay of PL and free hole absorption in the time range under study proceeds at the same rate (see Fig. 3). This rate is determined by thermal excitation of trapped electrons. The electrons detrapped into the conduction band either reach Ce^{3+} and recombine radiatively resulting in PL or are captured by nonradiative recombination centers and nonradiatively recombine with the holes in the valence band (their density is probed in FCA experiment). Thus, the rates of both processes depend on the population of free electrons in the same sink –the conduction band. As might be traced in Fig. 3 (see the lines depicting the bi-exponential fits of the experimental FCA transients presented by points), the codoping with magnesium slightly influences the decay rate: the decay time equals 3 ns in GAGG:Ce and 850 ps in GAGG:Ce,Mg and in the limits of experimental error does not depend on excitation wavelength.

The initial part of the time evolution of the density of free holes is presented in the inset of Fig. 4. As reported before, the PL intensity reaches the peak value within a few picoseconds after the short-pulse excitation. Note that the rise time of FCA signal in GAGG:Ce is by approximately three orders of magnitude shorter than that of the PL signal. Meanwhile, the FCA rise time in GAGG:Ce,Mg is in picosecond domain, shorter than the time resolution, which was limited in our pump and probe experiment by the pulse lengths of the beams (200 fs).

The discrepancy between the kinetics of free hole density and the time evolution of PL response evidences importance of excitation migration. Since the holes appear in the valence band (are observable in FCA) within several picoseconds even in GAGG:Ce without co-doping, that is the electronic part of the excitation that determines the recombination dynamics in this material. Trapping of electrons in host traps is highly probable in GAGG due to a considerable structural disorder and atomistic-scale composition fluctuations expected in this mixed garnet

crystal. Thus, the rise time of luminescence in GAGG:Ce is probably determined by the time, which is necessary to establish equilibrium in the electron exchange between the traps and Ce^{3+} ions acting as radiative recombination centers. Co-doping by Mg partially facilitates the transfer of the electrons to Ce^{3+} radiation centers, however, in parallel, it provides an effective channel for nonradiative recombination. As a result, the rise time of PL response in GAGG:Ce,Mg becomes considerably shorter than that in the crystal without codoping (has no slow component, which is present in the crystal without codoping), while the light yield only slightly decreases. The enhancement of the transfer rate might also be caused by the stabilization of Ce^{4+}, which favors the immediate trapping of free electrons from conduction band by the stable Ce^{4+} ions followed by Ce^{3+} emission [22,23]. Anyway, the enhancement enables the immediate build-up of photoluminescence and scintillation responses with negligible rise time.

4. Conclusions

Co-doping of GAGG:Ce by magnesium decreases the rise time of luminescence after short-pulse excitation down to sub-picosecond domain. This short response time is beneficial for the exploitation of the luminescence rise edge for fast timing in scintillation detectors. The fast rising edge of luminescence response enables determination of the time, when the luminescence intensity reaches a certain level, with sub-picosecond accuracy irrespectively of the total height of the luminescence response pulse. The Mg co-doping decreases the light yield of GAGG:Ce by ∼20%, however, the light yield of GAGG:Ce,Mg is still high enough (27,000 ph/MeV in the sample under this study) to be competitive in many applications. The holes become active in free carrier absorption within sub-picosecond time in GAGG:Ce,Mg and within few picoseconds in GAGG:Ce. Meanwhile, the final rise in GAGG:Ce luminescence intensity takes a few nanoseconds even at the resonant excitation of Ce^{3+} ions into $5d^2$ level situated in the host conduction band. This feature is caused by efficient transfer of electrons from $5d^2$ level to host trapping centers. The introduction of magnesium facilitates the transfer of electrons to Ce^{3+} and results in the decrease of the luminescence rise time down to sub-picosecond domain. The magnesium-related substantial decrease in the luminescence rise time at a modest decrease in the light yield evidences that GAGG:Ce,Mg is a promising scintillating material for many applications, where the time resolution by an order of magnitude shorter than that in the currently conventional scintillator-based detectors is required.

References

[1] P. Lecoq, M. Korzhik, A. Vasiliev, Can transient phenomena help improving time resolution in scintillators, IEEE Trans. Nucl. Sci. 61 (2014) 229–234. http://dx.doi.org/10.1109/TNS.2013.2282232.

[2] M. Harrison, International Linear Collider Technical Design Report, Vols. 1 through 4, 2013. http://inis.iaea.org/Search/search.aspx?orig_q=RN:45110508 (accessed October 20, 2016).

[3] W.W. Moses, Time of flight in PET revisited, IEEE Trans. Nucl. Sci. 50 (2003) 1325–1330. http://dx.doi.org/10.1109/TNS.2003.817319.

[4] C. Fong, A.W. Dong, A.J. Hill, B.J. Boyd, C.J. Drummond, Positron annihilation lifetime spectroscopy (PALS): a probe for molecular organisation in self-assembled biomimetic systems, Phys. Chem. Chem. Phys. 17 (2015) 17527–17540. http://dx.doi.org/10.1039/C5CP01921D.

[5] D.R. Schaart, E. Charbon, T. Frach, V. Schulz, Advances in digital SiPMs and their application in biomedical imaging, Nucl. Instrum. Methods Phys. Res. A 809 (2016) 31–52. http://dx.doi.org/10.1016/j.nima.2015.10.078.

[6] P. Lecoq, A. Annenkov, A. Gektin, M. Korzhik, C. Pedrini, Inorganic Scintillators for Detector Systems, Springer, 2006, p. 256.

[7] M.V. Nemallapudi, S. Gundacker, P. Lecoq, E. Auffray, A. Ferri, A. Gola, et al., Sub-100 ps coincidence time resolution for positron emission tomography with LSO:Ce codoped with Ca, Phys. Med. Biol. 60 (2015) 4635–4649. http://dx.doi.org/10.1088/0031-9155/60/12/4635.

[8] D.N. ter Weele, D.R. Schaart, P. Dorenbos, Intrinsic scintillation pulse shape measurements by means of picosecond X-ray excitation for fast timing applications, Nucl. Instrum. Methods Phys. Res. A 767 (2014) 206–211. http://dx.doi.org/10.1016/j.nima.2014.08.019.

[9] M. Kavatsyuk, D. Bremer, V. Dormenev, P. Drexler, T. Eissner, W. Erni, et al., Performance of the prototype of the Electromagnetic Calorimeter for PANDA, Nucl. Instrum. Methods Phys. Res. A 648 (2011) 77–91. http://dx.doi.org/10.1016/j.nima.2011.06.044.

[10] S. Gundacker, E. Auffray, K. Pauwels, P. Lecoq, Measurement of intrinsic rise times for various L(Y)SO and LuAG scintillators with a general study of prompt photons to achieve 10 ps in TOF-PET, Phys. Med. Biol. 61 (2016) 2802–2837. http://dx.doi.org/10.1088/0031-9155/61/7/2802.

[11] E. Auffray, R. Augulis, A. Borisevich, V. Gulbinas, A. Fedorov, M. Korjik, et al., Luminescence rise time in self-activated $PbWO_4$ and Ce-doped $Gd_3Al_2Ga_3O_{12}$ scintillation crystals, J. Lumin. 178 (2016) 54–60. http://dx.doi.org/10.1016/j.jlumin.2016.05.015.

[12] K. Kamada, T. Yanagida, J. Pejchal, M. Nikl, T. Endo, K. Tsutsumi, et al., Crystal growth and scintillation properties of Ce doped $Gd_3(Ga,Al)_5O_{12}$ single crystals, IEEE Trans. Nucl. Sci. 59 (2012) 2112–2115. http://dx.doi.org/10.1109/TNS.2012.2197024.

[13] K. Kamada, M. Nikl, S. Kurosawa, A. Beitlerova, A. Nagura, Y. Shoji, et al., Alkali earth co-doping effects on luminescence and scintillation properties of Ce doped $Gd_3A_{12}Ga_3O_{12}$ scintillator, Opt. Mater. 41 (2015) 63–66. http://dx.doi.org/10.1016/j.optmat.2014.10.008.

[14] M.T. Lucchini, V. Babin, P. Bohacek, S. Gundacker, K. Kamada, M. Nikl, et al., Effect of Mg^{2+} ions co-doping on timing performance and radiation tolerance of Cerium doped $Gd_3A_{12}Ga_3O_{12}$ crystals, Nucl. Instrum. Methods Phys. Res. A 816 (2016) 176–183. http://dx.doi.org/10.1016/j.nima.2016.02.004.

[15] M.T. Lucchini, S. Gundacker, P. Lecoq, A. Benaglia, M. Nikl, K. Kamada, A. Yoshikava, E. Auffray, Timing capabilities of garnet crystals for detecion of high energy charged particles, Nucl. Instrum. Methods Phys. Res. A 852 (2017) 1–9. http://dx.doi.org/10.1016/j.nima.2017.02.009.

[16] M. Nikl, K. Kamada, V. Babin, J. Pejchal, K. Pilarova, E. Mihokova, et al., Defect engineering in Ce-doped aluminum garnet single crystal scintillators, Cryst. Growth Des. 14 (2014) 4827–4833. http://dx.doi.org/10.1021/cg501005s.

[17] Ji. Kvapil, Jo. Kvapil, B. Manek, B. Perner, R. Autrata, P. Shauer, Czochralski growth of YAG:Ce in reducing protective atmosphere, J. Cryst. Growth 52 (1981) 542–545. http://dx.doi.org/10.1016/0022-0248(81)90336-5.

[18] J.M. Ogiegło, A. Katelnikovas, A. Zych, T. Ju, A. Meijerink, C.R. Ronda, Luminescence and luminescence quenching in $Gd_3(Ga,Al)_5O_{12}$ scintillators doped with Ce^{3+}, J. Phys. Chem. A 117 (2013) 2479–2484. http://dx.doi.org/10.1021/jp309572p.

[19] Y. Wu, F. Meng, Q. Li, M. Koschan, C.L. Melcher, Role of Ce^{4+} in the scintillation mechanism of codoped Gd3Ga3Al2 O12:Ce, Phys. Rev. Appl. 2 (2014) 1–13. http://dx.doi.org/10.1103/PhysRevApplied.2.044009.

[20] P. Dorenbos, Electronic structure and optical properties of the lanthanide activated RE3(Al1-xGax)5O12 (RE = Gd, Y, Lu) garnet compounds, J. Lumin. 134 (2013) 310–318. http://dx.doi.org/10.1016/j.jlumin.2012.08.028.

[21] E. Auffray, M. Korjik, M.T. Lucchini, S. Nargelas, O. Sidletskiy, G. Tamulaitis, et al., Free carrier absorption in self-activated $PbWO_4$ and Ce-doped $Y_3(Al_{0.25}Ga_{0.75})_3O_{12}$ and $Gd_3Al_2Ga_3O_{12}$ garnet scintillators, Opt. Mater. 58 (2016) 461–465. http://dx.doi.org/10.1016/j.optmat.2016.06.040.

[22] S. Blahuta, A. Bessiere, B. Viana, P. Dorenbos, V. Ouspenski, Evidence and Consequences of Ce in LYSO: Ce, Ca and LYSO: Ce, Mg single crystals for medical imaging applications, IEEE Trans. Nucl. Sci. 60 (2013) 3134–3141. http://dx.doi.org/10.1109/TNS.2013.2269700.

[23] M. Nikl, V. Babin, J. Pejchal, V.V. Laguta, M. Buryi, J.A. Mares, et al., The stable Ce^{4+} center: A new tool to optimize Ce-doped Oxide scintillators, IEEE Trans. Nucl. Sci. 63 (2016) 433–438. http://dx.doi.org/10.1109/TNS.2015.2495119.